INTERNATIONAL JOURNAL FOR NUMERICAL METHODS IN FLUIDS, VOL. 1, 323–346 (1981)

AN APPROXIMATELY DIVERGENCE-FREE 9-NODE VELOCITY ELEMENT (WITH VARIATIONS) FOR INCOMPRESSIBLE FLOWS

D. F. GRIFFITHS

Department of Mathematical Sciences, University of Dundee, Scotland

SUMMARY

Explicit basis functions are constructed for 9-node biquadratic velocity fields which guarantee that a weak form of the continuity equation is satisfied. The corresponding pressure approximations are either piecewise constant, piecewise linear or piecewise bilinear. These results are extended to give bases for bilinear velocity/piecewise constant pressure elements and also to some three-dimensional brick elements.

KEY WORDS Finite Element Incompressible Material Divergence-free Bases

INTRODUCTION

The Finite Element Method has been widely used in the last decade, with a mixed degree of success, for solving incompressible flows. The failure of certain mixed formulations, many of which are analysed in Reference 1, centres around the incompressibility condition and is brought about by the incompatibility of the finite element approximants chosen for the velocity and the pressure. It has been known for some time that these approximants must satisfy what is called the Babuska–Brezzi condition.[2,3,1] Because it is a condition that can be difficult to verify in practice, depending as it does on the grid as well as the approximants, greater emphasis is placed on identifying those elements (and the grids to which they are applied) for which it is satisfied.

In an important paper, Crouzeix and Raviart[4] present and analyse several suitable approximants on triangular elements. Following on from this work, a technique was developed by Griffiths[5,6] which enabled element level basis functions for velocities, based on these approximants, to be constructed which automatically satisfy an approximate form of the continuity equation. The emphasis in these papers was on triangular elements with but one example, using the 9-node biquadratic velocity, discussed briefly for square elements.[6] In this paper we shall describe how these techniques can be extended to construct similar element level basis functions for a hierarchy of spaces built from a 9-node approximation on quadrilateral elements. Examination of these approximately divergence-free basis functions reveals that the velocity is composed of small vortex-like structures each contained within one, two or four elements. This feature may be used to give a clearer understanding of the consequences of changes to either the pressure approximation or the shape of the elements.

In the next section we describe the necessary framework and specify the problem more precisely. The remainder of the paper is then in two main parts. The first part concerns the 9-node biquadratic element and examines, in turn, the approximately divergence-free basis

0271-2091/81/040323-24$02.40 *Received 23 April 1981*

on a uniform grid, the reductions possible to the number of degrees of freedom in the velocity, the application to Stokes' flow (with emphasis on the pressure calculation) and then the extensions of the earlier results to grids of quadrilateral elements. The second part then details the construction of an approximately divergence-free basis for the 4-node bilinear velocity element, firstly on uniform grids and then to perturbations of uniform grids.

STATEMENT OF THE PROBLEM

In the context of flow problems involving either the Stokes or Navier–Stokes equations on a two-dimensional region Ω, it is natural to take the velocity vector $\mathbf{q} = (u, v)^T$ to lie in the space $\mathbf{W}$ of vector valued functions which, together with their first partial derivatives, lie in $\mathbf{L}_2(\Omega)$. For the present we shall assume that each $\mathbf{q} \in \mathbf{W}$ vanishes on the boundary $\partial\Omega$ of Ω. The flow is said to be incompressible if $\mathbf{q}$ satisfies, at least in a weak sense, the continuity equation:

$$\operatorname{div} \mathbf{q} \equiv u_x + v_y = 0 \quad \text{in } \Omega. \tag{1}$$

It is well-known that any function $\mathbf{q} \in \mathbf{W}$ can be written as the sum of a curl (solenoidal part) and a gradient (irrotational part), i.e.

$$\mathbf{q} = \operatorname{curl} \psi + \operatorname{grad} \phi.$$

This implies that the space $\mathbf{W}$ can be split into two component parts:

$$\mathbf{W} = \mathbf{S} \oplus \mathbf{I} \tag{2}$$

where functions in $\mathbf{S}$ are solenoidal (satisfying (1)) and those in $\mathbf{I}$ are irrotational (satisfying $\operatorname{curl} \mathbf{q} = 0$). Therefore, from the entire space $\mathbf{W}$, only those vectors also belonging to $\mathbf{S}$ are candidates for the solution of the momentum equations. Functions in $\mathbf{S}$ are easily constructed by choosing a stream-function ψ and setting $\mathbf{q} = \operatorname{curl} \psi = (\psi_y, -\psi_x)^T$.

The problem addressed in this paper is that of how this framework can be carried over in a convenient and meaningful way to finite element spaces. An obvious way in which this can be done is to choose the stream-function ψ^h to be a $C^1(\Omega)$ finite element approximant and then set $\mathbf{q}^h = \operatorname{curl} \psi^h$. Two reasons for not adopting this approach are (i) C^1 approximants are notoriously difficult to construct on irregular grids of elements and (ii) we anticipate solving coupled equations (for example, the Stokes and continuity equations) and the 'optimal' solution, for a fixed number of degrees of freedom, occurs when both equations are satisfied to the same precision.

The region Ω is 'triangulated' into a number of polygonal elements to give a grid Ω^h where h is some notational measure of the diameter of the elements. We construct, on Ω^h, functions $\mathbf{q}^h$ which are continuous and which reduce to polynomials of fixed degree on each element. If some form of mapping is used to transform each element onto a reference element then $\mathbf{q}^h$ will be a polynomial on the reference element. The space, $\mathbf{W}^h$, comprising all such vector-valued functions is the counterpart of $\mathbf{W}$ described earlier.

Before we can describe the approximate form of (1) we must introduce an auxiliary space of finite element functions, Φ^h, called the pressure space. Functions in Φ^h are generally discontinuous at element boundaries and reduce to polynomials on each element (the degree being different to that for $\mathbf{W}^h$). A function $\mathbf{q}^h \in \mathbf{W}^h$ can now be said to be approximately divergence-free (or weakly solenoidal) if it satisfies

$$(\lambda^h, \operatorname{div} \mathbf{q}^h) = 0 \quad \text{for all} \quad \lambda^h \in \Phi^h \tag{3}$$

where $(.,.)$ is the usual L_2 inner product on Ω^h. The degree to which $\mathbf{q}^h$ satisfies the incompressibility constraint may be controlled by varying the dimension of the pressure space Φ^h.

The problem at hand can now be specified more precisely: it is to identify, from among all functions in $\mathbf{W}^h$, those functions which satisfy (3) for a given space Φ^h. These weakly solenoidal functions constitute a space $\mathbf{S}^h$ and we may write

$$\mathbf{W}^h = \mathbf{S}^h \oplus \mathbf{I}^h \tag{4}$$

where $\mathbf{I}^h$ is the complement of $\mathbf{S}^h$ in $\mathbf{W}^h$. Once $\mathbf{S}^h$ has been constructed, we can look for the solution of the Stokes equation (say) from among the functions in $\mathbf{S}^h$ rather than the larger space $\mathbf{W}^h$. Functions in $\mathbf{I}^h$, i.e. those in $\mathbf{W}^h$ but not in $\mathbf{S}^h$, do not enter into the calculation of the velocity but have a special role to play in the determination of the pressure as we shall later show. The dependence of $\mathbf{S}^h$ on both $\mathbf{W}^h$ and $\mathbf{\Phi}^h$ will usually be emphasized by writing $\mathbf{S}^h = \mathbf{S}^h(\mathbf{W}^h, \Phi^h)$ with a similar notation for $\mathbf{I}^h$.

AN APPROXIMATELY DIVERGENCE-FREE BIQUADRATIC BASIS

In this section Ω will refer to the unit square $(0, 1)\times(0, 1)$; generalizations to other quadrilateral elements will follow in a later section. The grid Ω^h is obtained by dividing Ω into N^2 equal square elements each of area h^2. The space $\mathbf{W}^h$ consists of all piecewise biquadratic functions on Ω^h which vanish on $\partial\Omega^h$ and which, on a typical element e (see Figure 1), may be expressed in the form

$$\mathbf{q}^h(x, y) = \sum_{j=0}^{8} \begin{pmatrix} U_j \\ V_j \end{pmatrix} \phi_j(x, y), \qquad (x, y) \in e \tag{5}$$

where $\{\phi_j\}$ are the usual (scalar) biquadratic shape functions on e. To distinguish the full biquadratic velocity (5) from variations to be introduced below, we write $\mathbf{W}^h = \mathbf{W}^h_{18}$ where the subscript refers to the number of degrees of freedom that the velocities enjoy on each element. Spaces $\mathbf{S}^h$ will be constructed, in turn, corresponding to each of the pressure spaces Φ^h_1, Φ^h_3 and Φ^h_4 where

$$\begin{aligned} &\Phi^h_1\text{: constant functions} \\ &\Phi^h_3\text{: linear functions} \quad \text{on each element.} \\ &\Phi^h_4\text{: bilinear functions} \end{aligned} \tag{6}$$

For $p^h \in \Phi^h_4$ we write

$$p^h = P\chi_1 + P_x\chi_2 + P_y\chi_3 + P_{xy}\chi_4 \quad \text{on } e \tag{7}$$

where the basis functions for the reference element $\hat{e} = \{-1 \le \xi, \eta \le 1\}$ are

$$\chi_1 = 1, \qquad \chi_2 = \xi, \qquad \chi_3 = \eta \quad \text{and} \quad \chi_4 = \xi\eta, \tag{8}$$

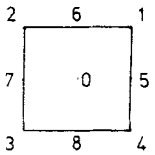

Figure 1. Nodes for the biquadratic approximant

and the nodal parameters P, P_x, P_y and P_{xy} are all identified with the node '0' in Figure 1. For $p^h \in \Phi_2^h$ set $P_{xy} = 0$ and, for $p^h \in \Phi_1^h$, set $P_x = P_y = P_{xy} = 0$.

The fact that each of the basis functions for the pressure space has support on a single element means that the incompressibility constraint (3) can be analysed one element at a time. For $\mathbf{S}^h(\mathbf{W}_{18}^h, \Phi_m^h)$, $m = 1, 3$ or 4, (3) takes the form

$$(\chi_j, \operatorname{div} \mathbf{q}^h)_e \equiv \iint_e \chi_j \operatorname{div} \mathbf{q}^h \, de = 0, \qquad j = 1, 2, \ldots, m \tag{9}$$

for each element $e \in \Omega^h$.

Consider first the case $m = 1$. Then $\mathbf{q}^h$ must satisfy, on each element e,

$$\iint_e \operatorname{div} \mathbf{q}^h \, de = 0. \tag{10}$$

On applying the Divergence Theorem, this becomes

$$\int_{\partial e} \mathbf{q}^h \cdot \mathbf{n} \, ds = 0 \tag{11}$$

where $\mathbf{n}$ is the unit outward normal vector to the boundary ∂e of e. Let s_k $(k = 1, 2, 3, 4)$ denote the side of ∂e which connects the kth node to the $(k+1)$st node (mod 4). Then (11) has a general solution which may be written in the form

$$\int_{s_k} \mathbf{q}^h \cdot \mathbf{n} \, ds = \psi_{k+1} - \psi_k, \qquad k = 1, 2, 3, 4, \tag{12}$$

with $\psi_5 \equiv \psi_1$ and the new nodal parameters $\{\psi_k\}$, one identified with each vertex, provide approximations to the stream-function at these points. The integral appearing on the left of (12) may be evaluated exactly by Simpson's rule to give

$$\begin{aligned} U_5 &= -\tfrac{1}{4}(U_1 + U_4) + \tfrac{3}{4}(\psi_1 - \psi_4)/h \\ V_6 &= -\tfrac{1}{4}(V_1 + V_2) + \tfrac{3}{4}(\psi_2 - \psi_1)/h \\ U_7 &= -\tfrac{1}{4}(U_2 + U_3) - \tfrac{3}{4}(\psi_3 - \psi_2)/h \\ V_8 &= -\tfrac{1}{4}(V_3 + V_4) - \tfrac{3}{4}(\psi_4 - \psi_3)/h. \end{aligned} \tag{13}$$

These equations, when substituted into (5), eliminate the 'normal velocity' component at each midside node and introduce the parameters ψ_j into the representation:

$$\mathbf{q}^h = \sum_{j=1}^{4} [U_j \boldsymbol{\phi}_j^u + V_j \boldsymbol{\phi}_j^v + \psi_j \boldsymbol{\phi}_j^\psi] + \begin{pmatrix} U_6\phi_6 + U_8\phi_8 + U_0\phi_0 \\ V_5\phi_5 + V_7\phi_7 + V_0\phi_0 \end{pmatrix} \tag{14}$$

in which $\boldsymbol{\phi}_j^u, \boldsymbol{\phi}_j^v$ and $\boldsymbol{\phi}_j^\psi$ are vector valued combinations of the original biquadratic basis functions. For example, on $\hat{e}$,

$$\begin{aligned} \boldsymbol{\phi}_1^u &= \begin{pmatrix} \phi_1 - \frac{1}{4}\phi_5 \\ 0 \end{pmatrix} = \tfrac{1}{8}\xi(1+\xi)(1+\eta)\begin{pmatrix} 3\eta - 1 \\ 0 \end{pmatrix}, \\ \boldsymbol{\phi}_1^v &= \begin{pmatrix} 0 \\ \phi_1 - \frac{1}{4}\phi_6 \end{pmatrix} = \tfrac{1}{8}\eta(1+\xi)(1+\eta)\begin{pmatrix} 0 \\ 3\xi - 1 \end{pmatrix}, \\ \boldsymbol{\phi}_1^\psi &= \frac{3}{4h}\begin{pmatrix} \phi_5 \\ -\phi_6 \end{pmatrix} = \frac{3}{8h}(1+\xi)(1+\eta)\begin{pmatrix} \xi(1-\eta) \\ -\eta(1-\xi) \end{pmatrix}. \end{aligned} \tag{15}$$

Equation (14) gives a local (element level) expression for a general function $\mathbf{q}^h \in \mathbf{S}^h(\mathbf{W}_{18}^h, \Phi_1^h)$, i.e. the biquadratic functions which satisfy the 'average mass balance' constraint (10) on each element. When contributions to $\mathbf{q}^h$ from all neighbouring elements are taken into account, its nodal parameters have associated basis functions whose support is contained on at most four elements. Representatives of the basis are sketched in Figure 2 where it may be seen that the basis function for ψ has a distinct vortex structure encircling the node and the remaining functions describe uni-directional flows. It is important to recognize that the expressions (13), written for a single element, are compatible with the analogous expressions for contiguous elements. This means in particular that they do not destroy the inter-element continuity of the global approximant.

We turn next to the construction of functions in $\mathbf{S}^h(\mathbf{W}_{18}^h, \Phi_3^h)$, i.e. those functions of the form (14) which satisfy the additional constraints

$$\iint_e \xi \operatorname{div} \mathbf{q}^h \, de = \iint_e \eta \operatorname{div} \mathbf{q}^h \, de = 0. \tag{16}$$

Integration by parts gives

$$\int_{\partial e} \xi \mathbf{q}^h \cdot \mathbf{n} \, ds - \iint_e u^h \, de = 0$$

and (17)

$$\int_{\partial e} \eta \mathbf{q}^h \cdot \mathbf{n} \, ds - \iint_e v^h \, de = 0$$

where $\mathbf{q}^h = (u^h, v^h)$. Evaluating these integrals by Simpson's rule and using (13) leads to

$$\begin{aligned} 4U_0 &= -U_6 - U_8 - \frac{3}{4}\sum_{j=1}^{4} (-1)^j V_j + \frac{3}{2}[\psi_1 + \psi_2 - \psi_3 - \psi_4]/h \\ 4V_0 &= -V_5 - V_7 - \frac{3}{4}\sum_{j=1}^{4} (-1)^j U_j - \frac{3}{2}[\psi_1 - \psi_2 - \psi_3 + \psi_4]/h. \end{aligned} \tag{18}$$

The required functions $\mathbf{q}^h \in \mathbf{S}^h(\mathbf{W}_{18}^h, \Phi_3^h)$ are obtained by substituting (18) into (14). The result is

$$\mathbf{q}^h = \sum_{j=1}^{4} [U_j \boldsymbol{\phi}_j^u + V_j \boldsymbol{\phi}_j^v + \psi_j \boldsymbol{\phi}_j^\psi] + V_5 \boldsymbol{\phi}_5^v + U_6 \boldsymbol{\phi}_6^u + V_7 \boldsymbol{\phi}_7^v + U_8 \boldsymbol{\phi}_8^u, \tag{19}$$

where we have used the same symbols, $\boldsymbol{\phi}_j^u$ etc., as in (14) but they now represent different functions. In place of (15) we find, again on $\hat{e}$,

$$\begin{aligned} \boldsymbol{\phi}_1^u &= \begin{pmatrix} \phi_1 - \frac{1}{4}\phi_5 \\ \frac{3}{16}\phi_0 \end{pmatrix} = \tfrac{1}{8}(1+\xi)(1+\eta)\begin{pmatrix} \xi(3\eta - 1) \\ \frac{3}{2}(1-\xi)(1-\eta) \end{pmatrix}, \\ \boldsymbol{\phi}_1^\psi &= \frac{3}{4h}\begin{pmatrix} \phi_5 + \frac{1}{2}\phi_0 \\ -\phi_6 - \frac{1}{2}\phi_0 \end{pmatrix} = \frac{3}{8h}(1+\xi)(1+\eta)\begin{pmatrix} 1-\eta \\ -1+\xi \end{pmatrix}, \\ \boldsymbol{\phi}_5^v &= \begin{pmatrix} 0 \\ \phi_5 - \frac{1}{4}\phi_0 \end{pmatrix} = \tfrac{1}{4}(1+\xi)(3\xi - 1)(1-\eta^2)\begin{pmatrix} 0 \\ 1 \end{pmatrix} \end{aligned} \tag{20}$$

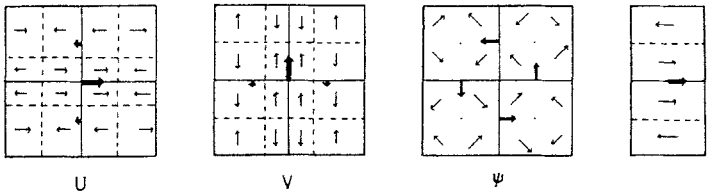

Figure 2. Sketches of the basis functions in $\mathbf{S}^h(\mathbf{W}_{18}^h, \Phi_1^h)$ associated with the parameters U, V and ψ (at a vertex) and the tangential velocity at a midside node. The velocity is zero along the broken lines and the bold arrows indicate velocities at nodes

as examples of the definitions of typical basis functions on a single element. The global nature of the basis functions is sketched in Figure 3 where it is seen that increasing the dimension of the pressure space has led to an improvement in the vortex structure of basis functions associated with vertex nodes whilst those associated with 'tangential' midside nodes remain uni-directional (cf. Figure 2).

The dimension of the pressure space may be increased still further by replacing Φ_3^h by Φ_4^h and gives rise to the weakly solenoidal space $\mathbf{S}^h(\mathbf{W}_{18}^h, \Phi_4^h)$. Functions in this space are obtanied from (19) by enforcing the additional constraint

$$\iint_e \xi\eta \operatorname{div} \mathbf{q}^h \, de = 0 \tag{21}$$

which, on integrating by parts, becomes

$$\int_{\partial e} \xi\eta \mathbf{q}^h \cdot \mathbf{n} \, ds = \iint_e (\eta u^h + \xi v^h) \, de. \tag{22}$$

This equation involves only boundary nodal values of $\mathbf{q}^h$. Application of Simpson's rule leads directly to the equation

$$V_5 - V_7 + U_6 - U_8 + \tfrac{1}{2}[-U_1 - V_1 - U_2 + V_2 + U_3 + V_3 + U_4 - V_4] = 0. \tag{23}$$

By grouping the terms in this equation into combinations involving tangential velocities along each edge, its general solution may be obtained in a manner similar to that for (11). Four new parameters $\sigma_1, \sigma_2, \sigma_3$ and σ_4 are introduced, one associated with each vertex of

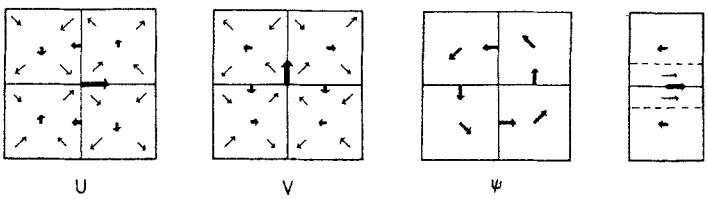

Figure 3. Sketches of the basis functions in $\mathbf{S}^h(\mathbf{W}_{18}^h, \Phi_3^h)$ associated with the parameters U, V and ψ at vertex nodes and the tangential velocity at a midside node

the element, through the relations

$$\begin{aligned} V_5 &= \tfrac{1}{2}(V_4 + V_1) + (\sigma_1 - \sigma_4)/4h, \\ U_6 &= \tfrac{1}{2}(U_1 + U_2) + (\sigma_2 - \sigma_1)/4h, \\ V_7 &= \tfrac{1}{2}(V_2 + V_3) - (\sigma_3 - \sigma_2)/4h, \\ U_8 &= \tfrac{1}{2}(U_3 + U_4) - (\sigma_4 - \sigma_3)/4h, \end{aligned} \tag{24}$$

which ensures that (23) is satisfied identically for all values of $\sigma_1, \sigma_2, \sigma_3$ and σ_4. The factor $4h$ is introduced in order that σ_j correspond to an approximation to $h^2\,\partial^2\psi/\partial x\,\partial y$ at the jth node and σ/h^2 converges to a finite limit as $h \to 0$. It is interesting to note that if the two values of σ on any edge of an element are the same, then the tangential velocity along that edge is a linear function. Consequently, σ is a measure of the departure from linearity of this velocity component along the edge. Substituting (24) into (19) eliminates the tangential velocity parameters at midside nodes and the result describes a general member of the space $\mathbf{S}^h(\mathbf{W}_{18}^h, \Phi_4^h)$:

$$\mathbf{q}^h = \sum_{i=1}^{4} [U_i \boldsymbol{\phi}_i^u + V_i \boldsymbol{\phi}_i^v + \psi_i \boldsymbol{\phi}_i^\psi + \sigma_i \boldsymbol{\phi}_i^\sigma] \tag{25}$$

where we have again used the same symbols ($\boldsymbol{\phi}_j^u$ etc.) to denote basis functions which are generally different to those in (14) and (19). In fact, typical basis functions are given by

$$\begin{aligned} \boldsymbol{\phi}_1^u &= \begin{pmatrix} \phi_1 - \frac{1}{4}\phi_5 + \frac{1}{2}\phi_6 - \frac{1}{8}\phi_0 \\ \frac{3}{16}\phi_0 \end{pmatrix} = \tfrac{1}{8}(1+\xi)(1+\eta)\begin{pmatrix} 3\eta - 1 \\ \frac{3}{2}(1-\xi)(1-\eta) \end{pmatrix} \\ \boldsymbol{\phi}_1^\psi &\text{ is identical to that in (15)} \\ \boldsymbol{\phi}_1^\sigma &= \frac{1}{4h}\begin{pmatrix} -\phi_6 + \frac{1}{4}\phi_0 \\ \phi_5 - \frac{1}{4}\phi_0 \end{pmatrix} = \frac{1}{16h}(1+\xi)(1+\eta)\begin{pmatrix} -(1-\xi)(3\eta - 1) \\ (1-\eta)(3\xi - 1) \end{pmatrix}. \end{aligned} \tag{26}$$

Their global counterparts are sketched in Figure 4. By adding the term $\xi\eta$ to the pressure on each element, the vortex structure of both U and V at vertices has been sharpened considerably, that for ψ remains unchanged and, what were previously uni-directional flows for tangential nodes, have now combined to give σ-basis functions having a vortex within each element. Comparison of Figures 2, 3 and 4 clearly shows the focusing effect that the pressure space has on the divergence-free properties of the element.

We feel that it is worth pointing out that the nodal parameters in (25) are the same as those which appear in the velocity, $\mathbf{q}_H^h$, derived as the curl of a stream-function based on

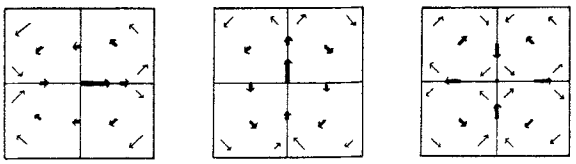

Figure 4. Sketches of the basis functions in $\mathbf{S}^h(\mathbf{W}_{18}^h, \Phi_4^h)$ associated with the parameters U, V and σ at vertex nodes

Hermite cubic elements on Ω^h. There are, however, two major differences between $\mathbf{q}_H^h$ and the velocity given by (25):

(i) $\mathbf{q}_H^h$ satisfies div $\mathbf{q}_H^h = 0$ whereas the expression (25) is only solenoidal in the sense of (9) with $m = 4$,

(ii) the basis functions in (25) are biquadratic whereas those for $\mathbf{q}_H^h$ are composed from functions which are cubic in one variable and quadratic in the other.

We shall show in a subsequent section that both these representations suffer from a common deficiency, namely, that neither is applicable on a grid of arbitrary quadrilateral elements.

We have now completed the description of all the decompositions of $\mathbf{W}_{18}$ which have a local basis. Any further increase in the dimension of the pressure space would no longer allow the construction of a basis by looking at a single element.

In the process of constructing the representations (14), (19) and (25) of functions in $\mathbf{S}^h(\mathbf{W}_{18}^h, \Phi_m^h)$, $m = 1, 3, 4$ respectively the independent degrees of freedom removed from $\mathbf{W}_{18}^h$ were

$$\mathbf{q}_1^h = U_5\begin{pmatrix}\phi_5\\0\end{pmatrix} + V_6\begin{pmatrix}0\\\phi_6\end{pmatrix} - U_7\begin{pmatrix}\phi_7\\0\end{pmatrix} - V_8\begin{pmatrix}0\\\phi_8\end{pmatrix}, \quad \text{(the normal velocities at midside nodes)} \tag{27}$$

$$\mathbf{q}_3^h = \mathbf{q}_1^h + \begin{pmatrix}U_0\\V_0\end{pmatrix}\phi_0, \quad \text{(centroid velocity)} \tag{28}$$

and

$$\mathbf{q}_4^h = \mathbf{q}_3^h + V_5\begin{pmatrix}0\\\phi_5\end{pmatrix} - U_6\begin{pmatrix}\phi_6\\0\end{pmatrix} - V_7\begin{pmatrix}0\\\phi_7\end{pmatrix} + U_8\begin{pmatrix}\phi_8\\0\end{pmatrix} \quad \text{(the tangential velocities at midside nodes)}$$

$$= \begin{pmatrix}U_0\\V_0\end{pmatrix}\phi_0 + \sum_{j=5}^{8}\begin{pmatrix}U_j\\V_j\end{pmatrix}\phi_j. \tag{29}$$

Now, whilst it is true that every function from $\mathbf{I}^h(\mathbf{W}_{18}^h, \Phi_m^h)$ is of the form $\mathbf{q}_m^h$, the converse is not, since, particular values of the nodal parameters in (27)–(29) give the basis functions $\boldsymbol{\phi}^\sigma$ and $\boldsymbol{\phi}^\psi$ which lie in $\mathbf{S}^h(\mathbf{W}_{18}^h, \Phi_m^h)$ (see, for example, equations (15), (20) and (26)). This property is unavoidable but, fortunately, can be used to advantage (see section on the Stokes equations). Note that the velocities in I^h are weakly irrotational in that $\iint_e \text{curl}\, \mathbf{q}^h \, de = 0$.

MODIFICATIONS OF THE BIQUADRATIC BASIS

The preceding section detailed the changes in the approximately divergence-free basis brought about by changes in the pressure space. We turn now to the question of how the biquadratic basis itself may be changed whilst maintaining both inter-element continuity and the divergence-free character. The dimension of the velocity approximation may be reduced by using a technique suggested by Griffiths[5,6] whereby the tangential velocity is constrained to be linear along each edge of an element whilst the variation in the normal velocity remains quadratic. For the element shown in Figure 1 the relevant reduction can by accomplished by setting $\sigma_j = 0$ $(j = 1, 2, 3, 4)$ in equations (24). The space of velocity functions which results when these expressions are substituted into (5) will be denoted by $\mathbf{W}_{14}^h$ since each function now has fourteen degrees of freedom on each element.

To construct the weakly solenoidal space $\mathbf{S}^h(\mathbf{W}_{14}^h, \phi_1^h)$ we simply substitute equations (24) (with $\sigma_j = 0$) into (14). The resulting basis functions (with the exception of the tangential

midside node which is now absent) differ only marginally from those depicted in Figure 2. The construction of $\mathbf{S}^h(\mathbf{W}^h_{14}, \Phi^h_3)$ is even more straightforward since it involves only the setting of $\sigma_j = 0$ $(j = 1, 2, 3, 4)$ in (25). Apart from the absence of the σ-basis function, the sketches shown in Figure 3 continue to apply (the remaining basis functions are identical in the two situations).

For the element shown in Figure 1, the velocity $\mathbf{q}^h = (u^h, v^h)^T \in \mathbf{W}^h_{14}$ is such that v^h is linear along edges 14 and 23 whilst u^h is linear along 12 and 34. This suggests that one way of removing the degrees of freedom associated with the node '0' is to assume that u^h is linear in x and v^h is linear in y throughout the entire element. This means setting

$$U_0 = \tfrac{1}{2}(U_5 + U_7) \quad \text{and} \quad V_0 = \tfrac{1}{2}(V_6 + V_8). \tag{30}$$

The number of degrees of freedom on the element is therefore reduced to twelve leading to the space $\mathbf{W}^h_{12}$. The only weakly solenoidal space that can be constructed on $\mathbf{W}^h_{12}$ is $\mathbf{S}^h(\mathbf{W}^h_{12}, \Phi^h_1)$ using piece-wise constant pressures. Typical functions on $\mathbf{S}^h(\mathbf{W}^h_{12}, \Phi^h_1)$ may be constructed either directly using equations (13) or by substituting expressions (30) into the representation for $\mathbf{q}^h \in \mathbf{S}^h(\mathbf{W}^h_{14}, \Phi^h_1)$.

The various weakly solenoidal functions which can be constructed from either $\mathbf{W}^h_{18}$ or the reduced biquadratic spaces $\mathbf{W}^h_{14}, \mathbf{W}^h_{12}$ are listed in Table I along with the transformations which connect them. The relative dimensions of these spaces can be assessed in terms of the *average number of parameters per element*. For example, $\mathbf{q}^h \in \mathbf{W}^h_{18}$ has a total of $2(2N-1)^2$ parameters on Ω^h and, consequently, $2(2N-1)^2/N^2$ parameters per element. For large values of N this gives an asymptotic value of eight parameters per element. Likewise, $\mathbf{W}^h_{14}$ and $\mathbf{W}^h_{12}$ have an average of six and four parameters per element respectively. The asymptotic dimensions of all the possible spaces are given in Table II.

The data in Table II serves as a useful guide when these elements are used, for example, to solve the Stokes equations (see next section). If N_1, N_2 and N_3 denote, respectively, the average number of parameters per element for $\mathbf{W}^h, \Phi^h$ and $\mathbf{S}^h(\mathbf{W}^h, \Phi^h)$ then the Lagrange multiplier formulation leads to a system of linear algebraic equations (in velocity and pressure) of dimension proportional to $N_1 + N_2$. When the same elements are made weakly solenoidal by constructing $\mathbf{S}^h(\mathbf{W}^h, \Phi^h)$, the dimension of the algebraic system (for velocity only) is proportional to N_3, the constant of proportionality being the same in both cases.

Table I. The underlying velocity spaces $\mathbf{W}^h_{18}$, $\mathbf{W}^h_{14}$ and $\mathbf{W}^h_{12}$ and the various approximately divergence-free spaces that can be constructed from them

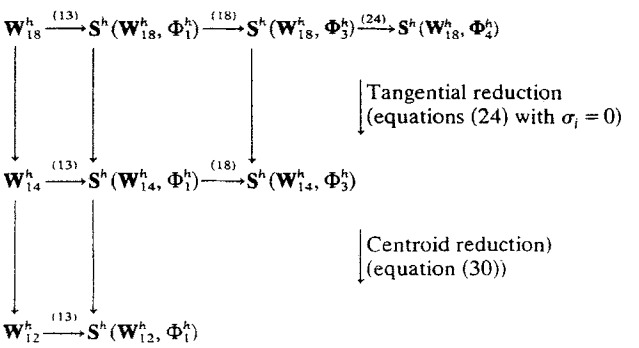

Table II. The average number of parameters per element for the various spaces, given in the form $\begin{matrix} N_1+N_2 \\ N_3 \end{matrix}$ where N_1, N_2 and N_3 are the average numbers for $\mathbf{W}^h$, Φ^h and $\mathbf{S}^h(\mathbf{W}^h, \Phi^h)$ respectively.

	Φ_1^h	Φ_3^h	Φ_4^h
$\mathbf{W}_{18}^h$	$\begin{matrix} 8+1 \\ 7 \end{matrix}$	$\begin{matrix} 8+3 \\ 5 \end{matrix}$	$\begin{matrix} 8+4 \\ 4 \end{matrix}$
$\mathbf{W}_{14}^h$	$\begin{matrix} 6+1 \\ 5 \end{matrix}$	$\begin{matrix} 6+3 \\ 3 \end{matrix}$	
$\mathbf{W}_{12}^h$	$\begin{matrix} 4+1 \\ 3 \end{matrix}$		

Thus, the ratio $N_3/(N_1+N_2)$, which ranges from $\frac{7}{9}$ down to $\frac{1}{3}$, gives an estimate for the reduction in the overall number of degrees of freedom in the system made possible by ensuring that the elements are weakly solenoidal at the outset.

A more physical interpretation of the data in Table II is that, of the available (N_1) degrees of freedom in the velocity, N_2 are absorbed into satisfying the incompressibility constraint leaving N_3 degrees of freedom with which to solve the momentum equations. One may conjecture that the spaces $\mathbf{W}^h$ and Φ^h are 'balanced' if N_2 and N_3 are nearly equal; this occurs when using either Φ_3^h or Φ_4^h. With only piecewise constant pressures (Φ_1^h), the ratio $N_3 : N_2$ is at best 3:1 which would seem to us to be too unbalanced.

SOLUTION OF THE STOKES EQUATIONS

In Stokes flow, the velocity ($\mathbf{q}$) and the pressure (p) satisfy the equations

$$-\nabla^2\mathbf{q} + \text{grad } p = \mathbf{f} \quad \text{in } \Omega, \tag{31}$$

$$\text{div } \mathbf{q} = 0 \quad \text{in } \Omega \tag{32}$$

and

$$\mathbf{q} = \mathbf{0} \quad \text{on } \partial\Omega. \tag{33}$$

We have chosen to use homogeneous boundary data only for definiteness at this point; we shall, at the opportune time, also describe the treatment of alternative boundary conditions.

If we define the bilinear form

$$a(\mathbf{w}, \mathbf{q}) = \iint_\Omega [\text{grad } w_1 \cdot \text{grad } q_1 + \text{grad } w_2 \cdot \text{grad } q_2] \, d\Omega \tag{34}$$

for $\mathbf{q} = (q_1, q_2)^T$ and $\mathbf{w} = (w_1, w_2)^T$, then the Lagrange Multiplier formulation of the finite element solution of (31)–(33) takes the form

Find $\mathbf{q}^h \in \mathbf{W}^h$ and $p^h \in \Phi^h$ such that

$$a(\mathbf{w}^h, \mathbf{q}^h) - (\text{div } \mathbf{w}^h, p^h) = (\mathbf{w}^h, \mathbf{f}), \quad \text{for all} \quad \mathbf{w}^h \in \mathbf{W}^h \tag{35}$$

and

$$(\lambda^h; \operatorname{div} \mathbf{q}^h) = 0 \quad \text{for all} \quad \lambda^h \in \Phi^h. \tag{36}$$

It is well known that both the continuous and discrete systems also require that the pressure be specified at one point in Ω in order that the solutions be unique. The relationship between the Lagrange multiplier equations (35), (36) and certain penalty methods using reduced integration is explored by Sani *et al.*[1]

If the approximately divergence-free forms of the space $\mathbf{W}^h$ are used, equations (35) and (36) are replaced by:

Find $\mathbf{q}^h \in \mathbf{S}^h(\mathbf{W}^h, \Phi^h)$ such that

$$a(\mathbf{w}^h, \mathbf{q}^h) = (\mathbf{w}^h, \mathbf{f}) \quad \text{for all} \quad \mathbf{w}^h \in \mathbf{S}^h(\mathbf{W}^h, \Phi^h). \tag{37}$$

In this way the computation of the velocity is completely separated from that of the pressure. Because the functions in $\mathbf{S}^h(\mathbf{W}^h, \Phi^h)$ have been given explicitly on each element, the normal procedures for assembling finite element equations may be used. The linear independence of the basis functions together with the ellipticity of $a(.,.)$ ensures that the coefficient matrix arising from (37) is positive definite. The resulting linear algebraic equations consequently have a unique solution which, when solved by direct elimination methods, require no pivoting.

Once the velocity has been computed from (37), the pressure follows from the equations

$$(\operatorname{div} \mathbf{w}^h, p^h) = a(\mathbf{w}^h, \mathbf{q}^h) - (\mathbf{w}^h, \mathbf{f}) \tag{38}$$

where $\mathbf{w}^h$ ranges over functions which are in $\mathbf{W}^h$ but not in $\mathbf{S}^h(\mathbf{W}^h, \Phi^h)$, i.e. over all $\mathbf{w}^h \in \mathbf{I}^h$. Such functions are listed in equations (27)–(29).

To describe the pressure process in more detail, we consider the patch of four elements shown in Figure 5 and each of the pressure spaces Φ^h_m, $m = 1, 3, 4$ in turn.

The pressure $p^h \in \Phi^h_1$

p^h is a constant on each element of the patch and we denote by P_j its value on the jth element. Suitable vectors $\mathbf{w}^h$ are given in equation (27); we begin by taking $\mathbf{w}^h = (\phi_1, 0)^T$ (ϕ_1 is the usual biquadratic basis function for the node M_1 of Figure 5). In this form, $\mathbf{w}^h$ is normal to the edge at M_1; this is not essential, the only proviso is that $\mathbf{w}^h$ should not be parallel to the edge for then it would belong to $\mathbf{S}^h(\mathbf{W}^h, \Phi^h_1)$. The pressure calculation is virtually identical for each of the velocity spaces $\mathbf{W}^h_{18}$, $\mathbf{W}^h_{14}$ and $\mathbf{W}^h_{12}$ so we shall suppress the subscript and write simply $\mathbf{W}^h$. With $\mathbf{w}^h = (\phi_1, 0)^T$ equation (38) becomes

$$(P_1 - P_2)h = a(\mathbf{w}^h, \mathbf{q}^h) - (\mathbf{w}^h, \mathbf{f}) \tag{39}$$

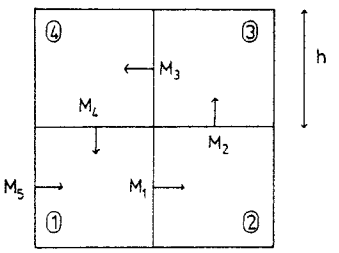

Figure 5. A patch of four elements for describing the calculation of the pressure approximation

from which P_2 may be computed in terms of P_1. Repeating this process with $\mathbf{w}^h = (0, \phi_2)^T, (-\phi_3, 0)^T$ and $(0, -\phi_4)^T$ allows the calculation of $P_2 - P_3$, $P_3 - P_4$ and $P_4 - P_1$ respectively. Therefore, starting with any given value for P_1 (the hydrostatic level), we can use these four equations to determine, in turn, the values of P_2, P_3, P_4 and then P_1. It is clearly essential that the original and final values for P_1 should agree. Reference to equations (14) and (15) reveals that the sum of the four $\mathbf{w}^h$ functions so chosen combine to form the basis function $\boldsymbol{\phi}^\psi \in \mathbf{S}^h(\mathbf{W}^h, \Phi_1^h)$. The sum of the four equations derived for the pressures therefore gives equation (37) with $\mathbf{w}^h = \boldsymbol{\phi}^\psi$. The values of the pressure are therefore consistent. By extending this marching process to the entire grid, the pressure may be found on each element in terms of the arbitrary (hydrostatic) value chosen in the first element. In the terminology of Sani *et al.*,[1] this element exhibits a hydrostatic pressure mode. Precisely the same process applies if $\mathbf{q}$ assumes non-zero values on $\partial\Omega$ (see (33)). There should perhaps be a word of caution regarding the way in which these boundary values are incorporated into $\mathbf{q}^h$. To ensure overall consistency, the net mass flux of $\mathbf{q}^h$ across $\partial\Omega^h$ should agree with that of $\mathbf{q}$, i.e.

$$\int_{\partial\Omega} \mathbf{q} \cdot \mathbf{n}\, ds = \int_{\partial\Omega} \mathbf{q}^h \cdot \mathbf{n}\, ds. \tag{40}$$

When applying the boundary conditions to $\mathbf{q}^h$, values at vertex nodes and tangential components at midside nodes are interpolated in the usual way. The normal component of $\mathbf{q}^h$ on an element edge, E (lying on $\partial\Omega^h$), is determined from

$$\int_E \mathbf{q}^h \cdot \mathbf{n}\, ds = \int_E \mathbf{q} \cdot \mathbf{n}\, ds \tag{41}$$

and the integral on the left may be evaluated by Simpson's rule. We have found that interpolation of the normal component of $\mathbf{q}$ along smooth edges of the boundary $\partial\Omega^h$ causes no ill effects, it is near corners (as, for example, in the driven cavity problem) that care has to be taken to match the fluxes across element edges. Note that (41), together with (12), determines the nodal values ψ_j on the boundary to within an arbitrary constant, which may be taken to be zero (if Ω also has an internal boundary, enclosing a 'hole', the nodal values of ψ are taken to be equal on it).

If the boundary conditions are altered so that the normal component of $\mathbf{q}$ is not specified on the entire boundary, for example, if it is not specified along the edge including node M_5 of Figure 5, then the vector $\mathbf{w}^h = (\phi_5, 0)^T$ enters the trial space $\mathbf{I}^h$. When this particular choice for $\mathbf{w}^h$ is substituted into (38) the value of P_1 is determined uniquely; the hydrostatic mode has been eliminated.

The pressure $p^h \in \Phi_3^h$

p^h now has the form

$$p^h = P_j + (x - x_j)P_{xj} + (y - y_j)P_{yj} \quad \text{on the } j\text{th element} \tag{42}$$

where (x_j, y_j) are the co-ordinates of the centroid of this element. It is seen from (28) that changing the pressure space from Φ_1^h to Φ_3^h introduces the two new functions $\mathbf{w}^h = (\phi_0, 0)^T$ and $(0, \phi_0)^T$ into the test space ('0' refers to the centre node of any element). Substituting these functions $\mathbf{w}^h$ into (38) leads to

$$-\tfrac{4}{9}h^2 P_{xj} = a(\mathbf{w}^h, \mathbf{q}^h) - (\mathbf{w}^h, \mathbf{f}), \qquad \mathbf{w}^h = (\phi_0, 0)^T \tag{43}$$

and

$$-\tfrac{4}{9}h^2 P_{yj} = a(\mathbf{w}^h, \mathbf{q}^h) - (\mathbf{w}^h, \mathbf{f}), \qquad \mathbf{w}^h = (0, \phi_0)^T \tag{44}$$

from which P_{xj} and P_{yj}, on element j, follow immediately. The difference in the hydrostatic levels $P_{j+1} - P_j$ between two adjacent elements is computed in the same manner as for Φ_1^h except that the analogue of equation (39) includes a known term involving $P_{xj+1} - P_{xj}$ (for a horizontal edge the additional term would involve P_y). Changes to the boundary conditions do not affect the computation of either P_x or P_y.

The pressure $p^h \in \Phi_4^h$.

p^h has the form

$$p^h = P_j + (x - x_j)P_{xj} + (y - y_j)P_{yj} + (x - x_j)(y - y_j)P_{xyj} \tag{45}$$

in the same notation as (42). It turns out that the equations which determine P_j, P_{xj} and P_{yj} are precisely the same as those for $P^h \in \Phi_3^h$, this means these parameters are completely independent of the values of the parameters P_{xy} on the grid. Inspection of (29) reveals that the P_{xy} parameters may be found from (38) where $\mathbf{w}^h$ ranges over all the tangential velocity basis functions at midside nodes. If, in the setup depicted in Figure 5, we take $\mathbf{w}^h = (0, \phi_1)^T$, it follows from (38) that

$$\frac{h^3}{9}(P_{xy1} - P_{xy2}) = a(\mathbf{w}^h, \mathbf{q}^h) - (\mathbf{w}^h, \mathbf{f}). \tag{46}$$

The structure of this equation is the same as (39) for the hydrostatic component and it follows that

(i) There is no way in which the value of P_{xy} can be determined in the first element. The value of P_{xy} in subsequent elements is obtained in terms of that in the first as the marching process is continued. This arbitrariness in P_{xy} is the manifestation of the so-called 'checkerboard' (CB) pressure mode that this element is known to have (note that the contribution that P_{xy} makes to the pressure p^h on each element has $\pm$ values at the 2×2 Gauss points). A 'pressure filter' is developed in Sani *et al.*[1] in order to remove the unwanted mode; in the context of the present formulation this is equivalent to setting $P_{xy} = 0$ in each element.

(ii) Using the fact that functions in $\mathbf{I}^h$ combine to form basis functions $\boldsymbol{\phi}^\psi$ and $\boldsymbol{\phi}^\sigma$ in $\mathbf{S}^h$, it can be shown that the values of P_{xy} on the grid are self-consistent.

(iii) If the boundary conditions are modified so that the tangential component is not specified at all points of the boundary (for example, the edge containing node M_5 in Figure 5) then $\mathbf{w}^h = (0, \phi_5)^T$ enters the test space and, when it is substituted into (38), the arbitrariness in the CB mode is removed by fixing the value of P_{xy1} uniquely.

THE EXTENSION TO QUADRILATERAL ELEMENTS

Up until now we have limited the discussion to a square element, not only because of the simplification that ensues, but also because we feel that the results may be useful in this form. When dealing with a more general quadrilateral element, e, (see Figure 6) a bilinear transformation is used to map it onto the reference element $\hat{e} = \{-1 \le \xi, \eta \le 1\}$ in the usual manner. We number the sides $s_1, \ldots, s_4$ of e as in (12) and we denote by $\mathbf{N}_j$ $(j = 1, 2, 3, 4)$ the outward normal vector to side s_j, normalized so that $|\mathbf{N}_j| = L_j$, the length of s_j.

The problem now is to determine whether or not analogues of the representations (14),

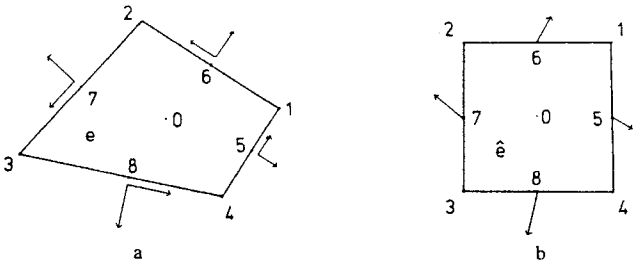

Figure 6. A general quadrilateral element (a) and the reference element (b). Also shown are the normal vectors $\mathbf{N}_j$ ($j = 5, 6, 7, 8$) before and after translation

(19) and (25) exist in this more general situation, or, equivalently, to determine whether the parameter transformations (13), (18) and (24) may be generalized in such a way as to preserve inter-element compatibility. A similar problem arises for triangular elements and has previously been resolved by Griffiths.[5,6]

Let $\mathbf{T}_j$ ($j = 1, 2, 3, 4$) denote the vector parallel to the side s_j, directed in a counter-clockwise direction and normalized so that $|\mathbf{T}_j| = L_j$. The heavy dependence on normal and tangential velocity components suggests that we use q^h_{Nj} and q^h_{Tj}, as the degrees of freedom at a midside node j in preference to the Cartesian components U_j and V_j; these parameters are related through

$$q^h_{Nj} = \begin{pmatrix} U_j \\ V_j \end{pmatrix} \cdot \mathbf{N}_j, \qquad q_{Tj} = \begin{pmatrix} U_j \\ V_j \end{pmatrix} \cdot \mathbf{T}_j. \tag{47}$$

Some caution has to be exercised since the outward normal at a side of one element is the inward normal to the contiguous element which shares that side. Similarly, the sense of the tangential vector is reversed. There is no difficulty if the vectors $\mathbf{N}_j$ and $\mathbf{T}_j$ are assigned unique senses on side s_j of the grid and the basis functions suitably modified by the inclusion of $\pm$ signs.

If $\{\phi_j(\xi, \eta)\}$ denote the usual biquadratic basis functions on $\hat{e}$, the basic representation of $\mathbf{q}^h \in \mathbf{W}^h_{18}$ is

$$\mathbf{q}^h = \sum_{j=0}^{4} \begin{pmatrix} U_j \\ V_j \end{pmatrix} \phi_j(\xi, \eta) + \sum_{j=5}^{8} (q_{Nj}\mathbf{N}_j + q_{Tj}\mathbf{T}_j)\phi_j(\xi, \eta)/L_j^2, \tag{48}$$

which reduces to (5) when e is square.

The spaces $\mathbf{S}^h(\mathbf{W}^h, \Phi^h_1)$

The 'average mass balance' equation on e, generated by piecewise constant pressures, is still given by (10). The general solution, obtained in an entirely similar vein to (12), is given by

$$q_{Nk} = -\tfrac{1}{4}(\mathbf{Q}_{k-4} + \mathbf{Q}_{k-5}) \cdot \mathbf{N}_k + \tfrac{3}{2}(\psi_{k-4} - \psi_{k-5}), \qquad k = 5, 6, 7, 8 \tag{49}$$

where $\mathbf{Q}_j = (U_j, V_j)^T$ ($j = 1, 2, 3, 4$), $\mathbf{Q}_0 = \mathbf{Q}_4$ and $\psi_0 = \psi_4$. Substitution of (49) into (48) gives the representation of $\mathbf{q}^h \in \mathbf{S}^h(\mathbf{W}^h_{18}, \Phi^h_1)$ which generalizes (14). It is a straightforward matter to verify that (49), for side s_k, is identical to the corresponding expression obtained by solving on the mass balance equations on a contiguous element which shares that side.

The tangential velocity can be constrained to be linear along each edge of e simply by requiring

$$q_{Tk} = \tfrac{1}{2}(\mathbf{Q}_{k-4} + \mathbf{Q}_{k-5}) \cdot \mathbf{T}_k, \qquad k = 5, 6, 7, 8. \tag{50}$$

Equation (48) together with (50) gives a general function in $\mathbf{W}_{14}^h$, whilst (48) with (49) and (50) represents a general function in $\mathbf{S}^h(\mathbf{W}_{14}^h, \Phi_1^h)$. We have not pursued the generalizations of $\mathbf{W}_{12}^h$.

The spaces $\mathbf{S}^h(\mathbf{W}^h, \Phi_3^h)$.

Equations (16) (or 17) continue to be the relevant forms of the additional constraint on a quadrilateral element e. By transforming the integrals on $\hat{e}$ and evaluating them by quadrature (Simpson's rule continues to give the exact values since the Jacobian of the transformation is bilinear in ξ and η on $\hat{e}$), expressions are obtained which may be solved for U_0 and V_0 in terms of the remaining parameters of the element. The appropriate constraints can, in this way, be satisfied on each element and lead to a representation of $\mathbf{q}^h \in \mathbf{S}^h(\mathbf{W}_{18}^h, \Phi_3^h)$ which takes the form (19) with V_5, U_6, V_7 and U_8 replaced by $q_{T5}, \ldots, q_{T8}$ respectively. Figures 2 and 3 now give only a general impression of the vortex structures on irregular grids. 'Tangential reduction' (the constraining of the tangential velocities to be linear) can be applied simply by substituting (50) into the representation of a general function from $\mathbf{S}^h(\mathbf{W}_{18}^h, \Phi_3^h)$; the result is a function in $\mathbf{S}^h(\mathbf{W}_{14}^h, \Phi_3^h)$.

The space $\mathbf{S}^h(\mathbf{W}_{18}^h, \Phi_4^h)$.

When the integral appearing in the constraint (21) (or 22) is evaluated it is found to depend solely on nodal parameters of $\mathbf{q}^h$ connected with the boundary nodes of e. Unfortunately, the coefficient of each boundary parameter involves, in general, properties of the element geometry which are not local to the side on which it lies (cf. equations (10) and (11)). This means that it is not, in general, possible to construct a general solution for (21) on e which would be compatible with similar solutions on contiguous elements. Although we cannot rule out the possibility that there may be particular irregular grids which would allow a local solution of (21), we believe that this constraint can only be satisfied, compatibly with neighbouring elements, if the mapping relating e to $\hat{e}$ is affine. Requiring the mapping to be affine would, in turn, restrict the grid to be composed entirely of parallelograms (including, of course, rectangular and square) elements. An appropriate solution can be indeed be constructed on such grids.

THE BILINEAR VELOCITY–PIECEWISE CONSTANT PRESSURE ELEMENT

We now examine a way in which the above technique for constructing weakly solenoidal basis functions can be applied to the 4-node velocity element. The technique that we have described is not immediately applicable because of the absence of midside nodes for this element. This difficulty is circumvented by considering a macro-element built from a patch of four neighbouring elements (Figure 7). The general principle applies equally to quadrilateral macro-elements though we shall consider only the case when they are square. There is no loss therefore in assuming that $e = \{-h \leq \xi, \eta \leq h\}$. The velocity, $\mathbf{q}^h$, on e is still given by the general form (5) but the basis functions $\{\phi_j\}$ are now piecewise bilinear on e. For example,

$$\phi_1 = \begin{cases} \xi\eta/h^2, & \text{in element '1'} \\ 0, & \text{in elements 2, 3 and 4.} \end{cases}$$

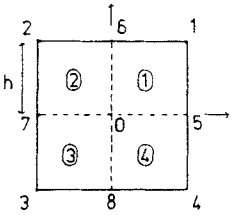

Figure 7. A macro-element, e, for the 4-node bilinear velocity

The conventional representation for the pressure on e would be in terms of the characteristic functions of each sub-element (i.e. the functions which take the value unity on one sub-element and zero on the remainder), but this is not convenient here. The techniques which were developed for the biquadratic element above can be applied directly if we choose the basis functions for Φ_4^h on e to be

$$\chi_1 = 1, \qquad \chi_2 = \operatorname{sgn} \xi, \qquad \chi_3 = \operatorname{sgn} \eta \quad \text{and} \quad \chi_4 = \chi_3 \chi_4, \tag{51}$$

where

$$\operatorname{sgn} \xi = \begin{cases} +1 & \text{for} \quad \xi > 0 \\ -1 & \text{for} \quad \xi < 0 \end{cases}$$

Employing the same symbols as before for the various function spaces, then the problem is to extract, from $\mathbf{W}_{18}^h$, an approximately divergence-free basis satisfying

$$\int\int_e \chi_j \operatorname{div} q^h \, de = 0, \qquad j = 1, 2, 3, 4. \tag{52}$$

Although it will prove possible to construct the analogues of all the spaces listed in Table I, our primary concern here is with the space $\mathbf{S}^h(\mathbf{W}_{18}^h, \Phi_4^h)$.

We shall exploit the similarity between (52) and (9) to the full. What we require, therefore, are the analogues of equations (13), (18) and (24). This involves a repetition of the previous construction with the obvious changes to the underlying basis functions $\{\phi_j\}$ and $\{\chi_k\}$. Integrals which were previously evaluated by Simpson's rule on (each edge of) e are now evaluated using the Trapezoidal rule on (each edge of) the sub-elements of e. The analogues of (13) and (18) can then be shown to be

$$\begin{aligned} U_5 &= -\tfrac{1}{2}(U_4 + U_1) + (\psi_1 - \psi_4)/h, \\ V_6 &= -\tfrac{1}{2}(V_1 + V_2) + (\psi_2 - \psi_1)/h, \\ U_7 &= -\tfrac{1}{2}(U_2 + U_3) - (\psi_3 - \psi_2)/h, \\ V_8 &= -\tfrac{1}{2}(V_3 + V_4) - (\psi_4 - \psi_3)/h, \end{aligned} \tag{53}$$

and

$$\begin{aligned} 2U_0 &= -U_6 - U_8 - \frac{1}{2}\sum_{j=1}^{4} (-1)^j V_j + [\psi_1 + \psi_2 - \psi_3 - \psi_4]/h, \\ 2V_0 &= -V_5 - V_7 - \frac{1}{2}\sum_{j=1}^{4} (-1)^j U_j - [\psi_1 - \psi_2 - \psi_3 + \psi_4]/h. \end{aligned} \tag{54}$$

Finally, it can be shown that the general solution of (52), with $j = 4$, is given by (24) (with no modifications). The 'tangential' and 'centre' reduction of $\mathbf{W}_{18}^h$ to $\mathbf{W}_{14}^h$ and $\mathbf{W}_{12}^h$ remain as before. By appropriate choices from among these expressions it is possible to construct bases for all the spaces listed in Table I.

We are particularly interested in the representation of functions in $\mathbf{S}^h(\mathbf{W}_{18}^h, \phi_4^h)$ so that we may use them in the next section. By substituting (53), (54) and (24) into (5) we obtain

$$\mathbf{q}^h = \sum_{j=1}^{4} [U_j \boldsymbol{\phi}_j^u + V_j \boldsymbol{\phi}_j^v + \psi_j \boldsymbol{\phi}_j^\psi + \sigma_j \boldsymbol{\phi}_j^\sigma]. \tag{55}$$

The vortex structure of each of the basis functions in (55) is depicted in Figure 4.

This element may be applied to the Stokes equation with no essential changes. The main conclusions remain valid and the most important of these are

(i) The pressure exhibits a spurious non-physical mode on a uniform grid. This mode, being due to the basis function χ_4, clearly has a checkerboard pattern: +1 on red squares and −1 on black squares. Application of the pressure 'filters' recommended in Reference 1 is equivalent to setting the coefficient of χ_4 to zero on each element.

(ii) There is, in general, no local basis for $\mathbf{S}^h(\mathbf{W}_{18}^h, \Phi_4^h)$ on an irregular grid of quadrilateral macro-elements. The obvious exceptions are grids of parallelograms although we believe, but have been unable to show, that a local basis can be found for grids satisfying the geometric condition (12) of Reference 1.

(iii) The arbitrary amplitude of the spurious CB pressure mode is removed if the boundary conditions are such that the tangential component of velocity is not prescribed at all points of the boundary.

Johnson and Pitkaranta[7] give a theoretical convergence analysis of the element when it is used for Stokes flows. They prove that if $\mathbf{q}^h \in \mathbf{S}^h(\mathbf{W}_{18}^h, \Phi_1^h)$ on a regular grid, then the velocities converge at the rate $O(h^2)$ and the pressure at $O(h)$, both results being for the respective L_2 norms.

THE 'TWEAKED' NODE PROBLEM

A problem is described by Sani *et al.*[1] in which one node, of an otherwise uniform partition of the unit square into N^2 square elements, is perturbed a distance $O(\varepsilon)$ where ε is small. It was discovered experimentally, and substantiated by a perturbation analysis, that when the bilinear velocity–piecewise constant pressure element was used to solve Stokes flow on this grid, small ε-perturbations (10^{-9}, 10^{-6} and 10^{-3}) to the grid could cause $O(1)$ and $O(\varepsilon^{-1})$ perturbations to the velocity and pressure fields respectively. In order to demonstrate the effects of this type of grid perturbation on the approximately divergence-free basis we consider a patch of four macro-elements as shown in Figure 8 wherein the co-ordinates of the centre 0 have been perturbed from (0, 0) to ($\varepsilon \cos\theta$, $\varepsilon \sin\theta$). It can be shown that $\mathbf{q}^h \in \mathbf{S}^h(\mathbf{W}_{18}^h, \Phi_4^h)$ satisfies the incompressibility constraints (52) on each of the macro-elements if

(i) it has the representation (55) on each macro-element ($\{\psi_j\}$ and $\{\sigma_j\}$ are defined by (53) and (24), as for square elements). The basis functions $\boldsymbol{\phi}_j^u$ etc. depend continuously on ε and θ,

and

(ii) $\mathbf{q}^h$ satisfies the further constraint (see also equation (67) of Reference 1)

$$\varepsilon \mathbf{N} \cdot (\mathbf{q}_9^h + \mathbf{q}_{11}^h - \mathbf{q}_{10}^h - \mathbf{q}_{12}^h) = 0 \tag{56}$$

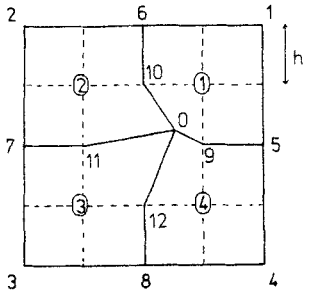

Figure 8. A patch of four macro-elements surrounding a 'tweaked' node

where $\mathbf{N} = (\sin\theta, -\cos\theta)$ is a unit vector perpendicular to the direction in which the node is displaced.

The constraint (56) clearly vanishes identically when $\varepsilon = 0$ but otherwise the parameters, and consequently the basis, must be adjusted in order to ensure its satisfaction. By defining $\mathbf{T} = (\cos\theta, \sin\theta)$ the general solution of (53) may be written in the form

$$\mathbf{q}_9^h + \mathbf{q}_{11}^h - \mathbf{q}_{10}^h - \mathbf{q}_{12}^h = \alpha\mathbf{T}, \quad \alpha \text{ arbitrary} \tag{57}$$

which, upon using the appropriate equations from (53) and (24), becomes

$$\begin{pmatrix} U_0 \\ -V_0 \end{pmatrix} = \frac{\alpha}{2}\begin{pmatrix} \cos\theta \\ \sin\theta \end{pmatrix} - \frac{1}{4}\sum_{j=5}^{8}\begin{pmatrix} U_j \\ -V_j \end{pmatrix} + \frac{1}{8h}\begin{pmatrix} \sigma_5 - \sigma_7 + 4\psi_6 - 4\psi_8 \\ \sigma_6 - \sigma_8 + 4\psi_5 - 4\psi_7 \end{pmatrix}. \tag{58}$$

When this expression is substituted into the velocity representation on the patch we obtain, for the most general function satisfying (52) on each macro-element,

$$\mathbf{q}^h = \alpha\boldsymbol{\phi}_0^\alpha + \sum_{j=1}^{8}\left[U_j\boldsymbol{\phi}_j^u + V_j\boldsymbol{\phi}_j^v + \psi_j\boldsymbol{\phi}_j^\psi + \sigma_j\boldsymbol{\phi}_j^\sigma\right] \tag{59}$$

where

$$\boldsymbol{\phi}_0^\alpha = \tfrac{1}{2}[\boldsymbol{\phi}_0^u\cos\theta - \boldsymbol{\phi}_0^v\sin\theta] \tag{60}$$

and the remaining basis functions $\boldsymbol{\phi}_j^u$ etc. are linear combinations of the earlier divergence-free bases for macro-elements. $\mathbf{q}^h$, as given by (59), is easily shown to be compatible with representations of the form (55) which hold for macro's outside this patch (for all values of ε and θ).

A number of important conclusions can be drawn from this representation.

(i) The velocity on the tweaked patch has one fewer degree of freedom compared to the velocity on an untweaked grid. By tweaking the centre node the two parameters U_0 and V_0 combine to give a single parameter α; it has only a local effect on the basis. The basis function $\boldsymbol{\phi}_0^\alpha$ represents a double vortex (cf. Figure 4 for U and V) with its axis parallel to the vector $(\cos\theta, -\sin\theta)$.

(ii) The effects on the velocity of tweaking a node for Stokes flow for a fixed value of h may be analysed by perturbation methods in linear algebra (see Reference 1). From such an analysis one can indeed conclude that an ε-perturbation to the grid can produce an $O(1)$ perturbation in the velocity unless the velocity on the untweaked grid also satisfies (56) with $\varepsilon \neq 0$, this is unlikely to occur if the grid is coarse.

(iii) The velocity on the tweaked grid is obtained by solving either (37) or the pair (35) and (36). In both cases the resulting field is represented by (59) on the patch and (58) can then be

used to deduce the velocity at the patch centre from the values of the parameters on the boundary of the patch. If the parameter values on the patch boundary are approximations of the corresponding continuous variables, then Taylor expansion of the right-hand side of (58) reveals that (U_0, V_0) converges to the required velocity at the centre provided that $\alpha \to 0$ as $h \to 0$ (the ratio ε/h must remain finite for otherwise the elements overlap). In fact, we obtain

$$\begin{pmatrix} U_0 \\ -V_0 \end{pmatrix} = \frac{\alpha}{2}\begin{pmatrix} \cos\theta \\ \sin\theta \end{pmatrix} + \begin{pmatrix} u \\ -v \end{pmatrix} - 2\begin{pmatrix} u - \psi_y \\ -v - \psi_x \end{pmatrix} + O(h^2) \tag{61}$$

where u, v and ψ are the continuous functions to which the boundary parameters are presumed to converge. Thus $(U_0, V_0) \to (u, v)$, as $h \to 0$, provided that $\mathbf{q} \equiv (u, v)^{\mathrm{T}} = \text{curl } \psi$ and $\alpha \to 0$. This analysis shows, for instance, that the interpolant to $\mathbf{q}$ from $\mathbf{S}^h(\mathbf{W}_{18}^h, \Phi_4^h)$ converges as $h \to 0$. The implication is that the $O(1)$ perturbation in ε referred to in (ii) is in fact an $O(h)O(1)$ perturbation as $h \to 0$. This behaviour has been observed in numerical experiments.[8]

The pressure for this problem is computed from (38) where $\mathbf{w}^h$ ranges over all functions in the complement of the approximately divergence-free space. Tweaking the node as we have seen removes one function from this divergence-free space and this has to be compensated for by adding one to the complement. The appropriate function is

$$\boldsymbol{\phi}_0 = \boldsymbol{\phi}_0^u \sin\theta + \boldsymbol{\phi}_0^v \cos\theta. \tag{62}$$

Without this function, equation (38) determines the pressure as for a uniform grid, that is to say, the coefficients of both P_1 and P_{xy1} are undetermined; there is a hydrostatic and a CB mode. Substituting (62) into (38) gives

$$-\tfrac{1}{2}\varepsilon \sum_{j=1}^{4} P_{xyj} = a(\boldsymbol{\phi}_0, \mathbf{q}^h) - (\boldsymbol{\phi}_0, \mathbf{f}) \tag{63}$$

which fixes the amplitude of the CB mode uniquely. If the grid perturbation causes only a small perturbation of the velocity (e.g. if the grid is fine enough) then, since $\boldsymbol{\phi}_0$ lies in the approximately divergence-free space on a uniform grid, the right-hand side of (63) is small by virtue of (37). The amplitude of the CB mode in this case may not, therefore, be unduly large. On the other hand, if the grid is too coarse, the grid perturbation leads to $O(1)$ changes in the velocity and the right-hand side of (63) is no longer small. One can expect therefore that the amplitude of the CB mode will be $O(\varepsilon^{-1})$.

The close parallel which exists between this macro-element and the 9-node biquadratic element suggests that the latter also has a similar behaviour on a tweaked grid. Finally, in this section, we note that this is not the only macro-element which can be analysed in this way. For example, each of the square sub-elements in Figure 7 could be split into two triangular sub-elements on which the velocity would be piecewise linear. The pressure field would continue to use the four basis functions (51) since it is well-known that the use of a pressure field which is piecewise constant on triangles leads to a locked system in which the constraints outnumber the degrees of freedom.

CONCLUSIONS

We have attempted, in this paper, to describe a new way of assessing and analysing finite element approximations to incompressible flows. The essential ingredient that we require, which is not new, is that the pressure approximation be defined independently on each

element. This creates jump discontinuities in the pressure across element boundaries (the pressure still lies in L_2) but it allows a local, element-level, basis to be constructed for weakly solenoidal velocity fields.

It is not, as yet, clear whether the computational procedures based on these basis functions would be more cost-effective than the orthodox Lagrange multiplier method (or indeed, penalty methods) although both methods would give identical results when used with the same underlying approximate function spaces. On the one hand, the use of an approximately divergence-free basis reduces the number of active degrees of freedom in the system (measured in terms of the dimension of the system of linear algebraic equations which have to be solved) by as much as a factor of three (see Table II) and, for Stokes' flows, the matrix of coefficients is symmetric positive-definite which therefore precludes the need for any form of pivoting in direct equation solvers. However, these features are, at least partly, offset by the fact that the bases are vector-valued functions and therefore, one presumes, more costly to implement (the actual number of such basis functions is fewer than for either the Penalty or the Lagrange multiplier method and it is, therefore, no foregone conclusion that our approach is more costly). The potential savings brought about by using these new basis functions are much greater for time dependent problems since the pressure does not need to be computed at each time step but only at those time levels that results are output. The elements can, of course, be implemented without change to the full Navier–Stokes equations.

A physically appealing feature of the basis functions we have constructed is that each represents a local 'vortex-like' structure supported on one, two or four contiguous elements (Figures 2, 3 and 4). Through these structures a clearer picture emerges of the effects of changing the pressure approximation and the shape of the elements. Another interesting feature is that it allows an interpretation to be assigned to the roles played by the various nodal parameters in the approximation: normal components of velocities at midside nodes control the flux across element edges (also the discontinuity in pressure across a boundary), internal nodes control the creation/destruction of mass within an element (also the gradient of the pressure in the element) and the remaining nodes are free to approximate the momentum equations.

By combining four elements to form a macro-element, we have been able to construct an approximately divergence-free basis for the 4-node bilinear velocity–piecewise constant pressure element. Although the basis has a local character, the fact that macro-elements are needed means that it cannot be expressed on a single element. By looking at small perturbations of regular grids we have been able to show that the macro-bilinear velocity-3-node pressure element (or, equivalently, the biquadratic velocity–*linear* pressure element) is relatively insensitive to such perturbations. However, increasing the number of pressure parameters per element to four can have dire consequences if the grid is not uniform (parallelograms) or if the grid is not sufficiently fine. This sensitivity to perturbations of the grid is not really so unusual. It can be likened to the failure of Hermite cubic elements to maintain inter-element continuity on irregular grids (using a bilinear mapping of quadrilateral elements onto the reference element). The equivalence of our approach to the Lagrange multiplier formulation using the same approximants means that these conclusions apply also to that scheme (and, to a lesser extent, to certain penalty methods with reduced integration[1]).

Since concluding this work, a recent paper by Fortin[9] has come to our attention in which, by a somewhat different route, he arrives at the same 'vortex-like' structure for describing the local flow. We take this as confirmation that this is indeed a good way to analyse finite element approximations of divergence-free flows. Briefly, the main difference in the

two approaches is in the way the element mass balance equation, (10), is satisfied. In our treatment, this is done by introducing a stream-function parameter at each vertex node whereas Fortin eliminates the normal component of velocity at a midside node by static condensation when two contiguous elements are assembled. Fortin goes further and examines several three-dimensional elements in a similar way. This has prompted us to extend our technique and an example of a three-dimensional element is presented in the Appendix.

APPENDIX

Three-dimensional elements

Let $\hat{e}$ denote the reference cube $\{-1 \leq \xi, \eta, \zeta \leq 1\}$ to which every cubic element in a regular grid Ω^h may be transformed by a translation and a scaling. The eight vertex nodes of $\hat{e}$ are numbered as shown in Figure 9 and the six faces of the cube $F_9, F_{10}, \ldots, F_{14}$ are labelled so they correspond, respectively, to the planes $\xi = +1, \eta = +1, \zeta = +1, \xi = -1, \eta = -1$, and $\zeta = -1$. Let $\mathbf{n}_j$ $(j = 9, \ldots, 14)$ denote the unit normal vector to face F_j oriented in the direction of one of the co-ordinate axes (e.g. $\mathbf{n}_{13} = (0, 1, 0)$). In the simplest of Fortin's 3D elements[9] $(Q_1^+ - P_0)$ the velocity in $\hat{e}$ is represented by its three Cartesian components at each vertex and by its normal velocity component on each face:

$$\mathbf{q}^h = \sum_{j=1}^{8} \begin{pmatrix} U_j \\ V_j \\ W_j \end{pmatrix} \phi_j(\xi, \eta, \zeta) + \sum_{j=9}^{14} \nu_j \tilde{\phi}_j(\xi, \eta, \zeta) \mathbf{n}_j \tag{64}$$

where $\{\phi_i\}$ are the usual trilinear basis functions for $\hat{e}$ and $\tilde{\phi}_j$ $(j = 9, \ldots, 14)$ is the 'bubble' function for the jth face F_j. For example,

$$\phi_1 = \tfrac{1}{8}(1+\xi)(1+\eta)(1+\zeta)$$

and

$$\tilde{\phi}_9 = \tfrac{1}{2}(1+\xi)(1-\eta^2)(1-\zeta^2).$$

Note that $\tilde{\phi}_9$ vanishes on all faces apart from F_9 and it takes the value unity at the ninth node. With this basis, the parameters ν_j are 'corrections' to the normal component of velocity at the centre of the jth face. For instance, the normal velocity at the ninth node, lying on F_9, is

$$\frac{1}{4} \sum_{j=1}^{4} U_j + \nu_9.$$

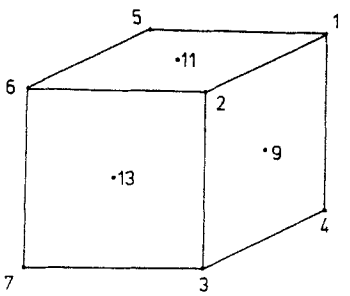

Figure 9. The reference element in 3D

When the pressure approximation is constant on each element, the velocity need only satisfy the element mass balance equation:

$$\iiint_e \operatorname{div} \mathbf{q}^h \, de = 0 \tag{65}$$

which integrates to give

$$\sum_{j=9}^{14} \iint_{F_j} \mathbf{q}^h \cdot \mathbf{n} \, ds = 0 \tag{66}$$

where $\mathbf{n}$ is the unit outward normal to $\hat{e}$ at F_j. To solve the analogous constraint (10) in two dimensions, we made use of the property of a stream-function: the difference between the values of the stream-function at two points A and B is equal to the flux across any curve joining A to B. In three dimensions the corresponding result is: the flux across any surface F (bounded by a closed curve Γ), is equal to the integral, taken around Γ, of the component of the stream-function $\boldsymbol{\psi}$ parallel to Γ. Applied to the contribution to (66) from F_9 for instance, this gives

$$\iint_{F_9} \mathbf{q}^h \cdot \begin{pmatrix} 1 \\ 0 \\ 0 \end{pmatrix} ds = \oint_{\partial F_9} \boldsymbol{\psi} \cdot \mathbf{t} \, dt \tag{67}$$

where $\mathbf{t}$ is a unit vector tangent to the boundary, ∂F_9, of F_9 directed counter-clockwise. If we now define $\mathbf{t}_{ij}$ to be a unit vector in the direction of the edge E_{ij} connecting the ith to the jth node, the right-hand side of (67) becomes

$$\int_{E_{12}} \boldsymbol{\psi} \cdot \mathbf{t}_{12} \, dt + \int_{E_{23}} \boldsymbol{\psi} \cdot \mathbf{t}_{23} \, dt + \int_{E_{34}} \boldsymbol{\psi} \cdot \mathbf{t}_{34} \, dt + \int_{E_{41}} \boldsymbol{\psi} \cdot \mathbf{t}_{41} \, dt.$$

There are now two (roughly equivalent) ways of proceeding. In the first of these we let α_{ij} denote an approximation to $\int_{E_{ij}} \boldsymbol{\psi} \cdot \mathbf{t}_{ij} \, dt$, for each i and j (note that $\alpha_{ij} = -\alpha_{ji}$). Now, evaluating the integral on the left of (67) using (64) gives, for F_9,

$$\sum_{j=1}^{4} U_j + \tfrac{16}{9} v_9 = \alpha_{12} + \alpha_{23} + \alpha_{34} + \alpha_{41}, \tag{68}$$

with a similar expression for each of the other faces. When these expressions are used to eliminate $v_9, \ldots, v_{14}$ from (64), we obtain, as the representation of a general function $\mathbf{q}^h$ on $\hat{e}$ satisfying (65),

$$\mathbf{q}^h = \sum_{j=1}^{8} \left[U_j \boldsymbol{\phi}_j^u + V_j \boldsymbol{\phi}_j^v + W_j \boldsymbol{\phi}_j^w + \sum_{\text{edges } E_{ij}} \alpha_{ij} \boldsymbol{\phi}_{ij}^\alpha \right] \tag{69}$$

in which

$$\boldsymbol{\phi}_1^u = (\phi_1 - \tfrac{9}{16}\tilde{\phi}_9, 0, 0)^T$$

$$\boldsymbol{\phi}_1^v = (0, \phi_1 - \tfrac{9}{16}\tilde{\phi}_{10}, 0)^T,$$

$$\boldsymbol{\phi}_1^w = (0, 0, \phi_1 - \tfrac{9}{16}\tilde{\phi}_{11})^T,$$

$$\boldsymbol{\phi}_{12}^\alpha = \tfrac{9}{16}(\tilde{\phi}_9, 0, -\tilde{\phi}_{11})^T$$

and the remaining basis functions are defined similarly. Of these basis functions, only those connected to 'α' parameters are not uni-directional. In fact $\boldsymbol{\phi}_{ij}^{\alpha}$ has a rudimentary vortex structure which encircles the edge E_{ij} (see Figure 10). The support of this basis function is the 2×2 block of elements which share the edge E_{ij}.

The representations (64) and (69) have, respectively, 30 and 36 parameters on each element but, on an assembled grid of elements, they both have an asymptotic average of six parameters per element.

In the representation (69), the parameter α_{ij} is a mid-edge node. Such nodes are often regarded unfavourably from a practical point of view. Mid-edge nodes may be avoided, however, provided we use approximations $\boldsymbol{\Psi}_k$ to the stream-function $\boldsymbol{\psi}$ at each vertex node k. A typical line integral from (67), $\int_{E_{ij}} \boldsymbol{\psi} \cdot \mathbf{t}_{ij}\, dt$ say, is approximated by $(\boldsymbol{\Psi}_i + \boldsymbol{\Psi}_j) \cdot \mathbf{t}_{ij}$ for each edge of $\hat{e}$. Thus, if $\boldsymbol{\Psi}_i = (\boldsymbol{\Psi}_i^1, \boldsymbol{\Psi}_i^2, \boldsymbol{\Psi}_i^3)^{\mathrm{T}}$, equation (68) is replaced by

$$\sum_{j=1}^{4} U_j + \tfrac{16}{9}\nu_9 = -(\boldsymbol{\Psi}_1^2 + \boldsymbol{\Psi}_2^2) - (\boldsymbol{\Psi}_2^3 + \boldsymbol{\Psi}_3^3) + (\boldsymbol{\Psi}_3^2 + \boldsymbol{\Psi}_4^2) + (\boldsymbol{\Psi}_4^3 + \boldsymbol{\Psi}_1^3). \tag{68'}$$

We should emphasize that (68) and (68′) (with their counterparts for the remaining faces) provide different, but equivalent, exact general solutions of (65) even though they involve approximations of line integrals. Both these general solutions are compatible with similar solutions on contiguous elements.

In contrast to (69), the approximately divergence-free velocity on $\hat{e}$ now has the form

$$\mathbf{q}^h = \sum_{j=1}^{8} \left\{ U_j \boldsymbol{\phi}_j^u + V_j \boldsymbol{\phi}_j^v + W_j \boldsymbol{\phi}_j^w + \sum_{k=1}^{3} \boldsymbol{\Psi}_j^k \boldsymbol{\phi}_j^k \right\} \tag{69'}$$

where the basis functions $\{\boldsymbol{\phi}_j^u\}$, $\{\boldsymbol{\phi}_j^v\}$ and $\{\boldsymbol{\phi}_j^w\}$ (for a single element) are the same as those in (69) and the '$\boldsymbol{\Psi}$' basis functions are simply related to those of the 'α' parameters in (69). For instance,

$$\boldsymbol{\phi}_1^2 = \boldsymbol{\phi}_2^2 = -\boldsymbol{\phi}_{12}^{\alpha}. \tag{70}$$

Although the form (69′) clearly involves 48 parameters on each element, asymptotically, the average number of parameters per element is the same as for (69). (Even though the 'element stiffness matrix' for (69′) is 48×48, it is effectively only 36×36 since, by virtue of (70), the remaining coefficients need only be copied into the correct positions.) For each component of $\boldsymbol{\Psi}$, the global basis functions are supported on the eight elements which meet at a vertex and represent twin vortices, each having the form shown in Figure 10, with their axes colinear.

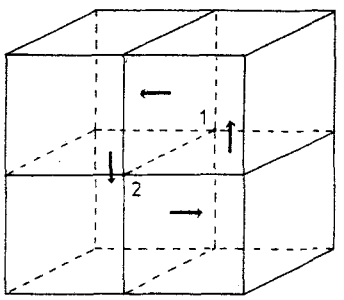

Figure 10. The vortex-like structure of $\boldsymbol{\phi}_{12}^{\alpha}$ (cf. Fortin,[9] Fig. 2.8)

By a similar process, element level basis functions may be constructed for all the 3D schemes proposed by Fortin.[9] In each case it is only the evaluation of the integrals on the left of (66) that require modification; the counterparts of (68) can still be used to eliminate the parameters $\{\nu_j\}$.

If the velocity (64) is supplemented by the term

$$(U_0, V_0, W_0)^{\mathrm{T}}(1-\xi^2)(1-\eta^2)(1-\zeta^2)$$

then the pressure approximation on $\hat{e}$ may be taken to be a linear function. The additional constraints

$$\int\int\int_{\hat{e}} \xi \operatorname{div} \mathbf{q}^h \, d\hat{e} = \int\int\int_{\hat{e}} \eta \operatorname{div} \mathbf{q}^h \, d\hat{e} = \int\int\int_{\hat{e}} \zeta \operatorname{div} \mathbf{q}^h \, d\hat{e} = 0$$

provide equations with which to eliminate the parameters U_0, V_0 and W_0 from the representation. The average number of parameters per element in this case is the same as for (69) and (69′), both of which only have piecewise constant pressures.

REFERENCES

1. R. L. Sani, P. M. Gresho, R. L. Lee, D. F. Griffiths and M. Engelman, 'The cause and cure (?) of the spurious pressures generated by certain FEM solutions of the incompressible Navier–Stokes equations; Parts I and II, *Int. J. Num. Meth. Fluids*, **1,** Nos. 1 and 2 (1981).
2. I. Babuska, 'Error bounds for finite element methods, *Numer. Math.*, **16,** 322–333 (1971).
3. F. Brezzi, 'On the existence, uniqueness and approximation of saddle-point problems arising from Lagrange multipliers, *R.A.I.R.O.*, **8-R2,** 129–151 (1974).
4. M. Crouzeix and P-A. Raviart, 'Conforming and non-conforming finite element methods for solving the stationary Stokes equations I', *R.A.I.R.O.*, **R-3,** 33–76 (1973).
5. D. F. Griffiths, 'Finite elements for incompressible flow', *Math. Meth. in Appl. Sci.*, **1,** 16–31 (1979).
6. D. F. Griffiths, 'The construction of approximately divergence-free finite elements', in *The Mathematics of Finite Elements and Applications III*, Academic Press, London, 1979, pp. 239–245.
7. C. Johnson and J. Pitkaranta, "Analysis of some mixed finite element methods related to reduced integration', Chalmers Univ. of Tech., *Comp. Sci. Report* 80.02 *R* (1980).
8. P. M. Gresho and R. L. Sani, Personal Communication.
9. M. Fortin, 'Old and new finite elements for incompressible flows', *Int. J. Num. Meth. Fluids*, **1,** 347–364 (1981).